Cell-autonomous activation of Hedgehog signaling inhibits brown adipose tissue development

LaGina Nosavanh[a,1], Da-Hai Yu[a], Eric J. Jaehnig[b], Qiang Tong[a], Lanlan Shen[a], and Miao-Hsueh Chen[a,2]

[a]United States Department of Agriculture/Agricultural Research Service Children's Nutrition Research Center, Department of Pediatrics, Baylor College of Medicine, Houston, TX 77030; and [b]Ludwig Institute for Cancer Research, Department of Cellular and Molecular Medicine, University of California School of Medicine, San Diego, La Jolla, CA 92093-0669

Edited by Yu-Hua Tseng, Joslin Diabetes Center, Harvard Medical School, Boston, MA, and accepted by the Editorial Board March 9, 2015 (received for review November 2, 2014)

Although recent studies have shown that brown adipose tissue (BAT) arises from progenitor cells that also give rise to skeletal muscle, the developmental signals that control the formation of BAT remain largely unknown. Here, we show that brown preadipocytes possess primary cilia and can respond to Hedgehog (Hh) signaling. Furthermore, cell-autonomous activation of Hh signaling blocks early brown-preadipocyte differentiation, inhibits BAT formation in vivo, and results in replacement of neck BAT with poorly differentiated skeletal muscle. Finally, we show that Hh signaling inhibits BAT formation partially through up-regulation of chicken ovalbumin upstream promoter transcription factor II (*COUP-TFII*). Taken together, our studies uncover a previously unidentified role for Hh as an inhibitor of BAT development.

Hedgehog signaling | brown adipose tissue | cell fate

Mammals possess two major types of adipose tissue: white adipose tissue (WAT) and brown adipose tissue (BAT). Although WAT stores energy as fat, BAT uses energy to generate heat by uncoupling mitochondrial oxidative phosphorylation (1). Traditionally, only small mammals and human infants were believed to possess functional BAT. However, various amounts of BAT have recently been discovered in healthy adult humans (2–4). Furthermore, recent observations that the thermal activity of human BAT can be increased by mild cold exposure suggest that promoting BAT activity may potentially serve as a therapeutic strategy for combating obesity (5, 6). Many research groups thus have identified genes that could potentially enhance the thermogenic activity of BAT in postnatal life (7, 8). However, two critical issues remain to be resolved: (*i*) understanding how BAT formation is controlled during development and (*ii*) identifying the postnatal reprogramming mechanisms that lead to the reduction/inactivation of the BAT in human adults.

BAT formation begins early in embryonic development. Recent lineage-tracing studies indicated that BAT, dermis, and skeletal muscle arise from the dermomyotome, a subset of the paraxial mesoderm (9, 10). The Hedgehog (Hh) signaling pathway is one of the major inductive signaling pathways controlling the patterning of paraxial mesoderm tissues. For example, Sonic Hh specifies and maintains epaxial muscle progenitor identity by activating *Myf5* and *MyoD* expression in the epaxial dermomyotome (11). Activation of the Hh pathway is initiated by external Hh ligand morphogens. In the absence of Hh ligand, the Hh receptor Patched (Ptch1) binds to Smoothened (Smo) and represses Hh pathway activity. Binding of Hh ligand to Ptch1 leads to activation of Smo, which converts the Gli transcription factors (Gli2 and -3) from repressors to activators, leading to expression of downstream target genes (12). These target genes include Hh-pathway components themselves; *Gli1* and *Ptch1* are the two direct Hh target genes most commonly used to evaluate Hh-pathway activation (12). Downstream of *Smo*, Gli-protein processing and activation is controlled by Suppressor of Fused (Sufu), and mouse embryos lacking Sufu show reductions in both the activator and repressor forms of Gli protein (13–15). Recently, a series of elegant studies indicated that core components of the Hh pathway localize to the primary cilium, a conserved cell-surface organelle, upon Hh stimulation in cultured cells and that the cilium plays an indispensable role in Hh-signal transduction (13, 16–18).

Although Hh signaling is important for the development of the paraxial mesoderm, the specific role of Hh signaling in BAT development is not clear. Pospisilik et al. concluded that Hh signaling regulates only WAT development because conditional *aP2-Sufu* knockout mice showed a reduction in WAT whereas BAT developed normally (19). However, in vitro and in vivo studies demonstrated that the Hh pathway is only submaximally activated by loss of Sufu because Sufu regulates both Gli activator and repressor protein stability (13, 14). Therefore, the phenotypes observed in *aP2-Sufu* knockout mice may not reflect the effects of maximal activation of the Hh pathway. Here, we show that brown preadipocytes contain primary cilia and are Hh-responsive. Furthermore, development of BAT is perturbed in *aP2-Cre; Ptch1*$^{flox/-}$ and *aP2-Cre; SmoM2* mice carrying maximal Hh-pathway activation. Finally, the Hh pathway inhibits brown-preadipocyte differentiation, partially via up-regulation of chicken ovalbumin upstream promoter transcription factor II (*COUP-TFII*).

Results

Differentiating Brown Adipocytes Are Ciliated and Respond to Hh Signal. To investigate the role of Hh signaling in BAT development, we first determined whether brown preadipocytes possess primary cilia in a commonly used brown-preadipocyte cell line, FVB-C3 (20). Strikingly, we found that primary cilia were present

Significance

The function of brown adipose tissue (BAT), which converts chemical energy into heat, has been widely characterized, but how BAT forms and what signaling molecules regulate its formation are largely unknown. In this paper, we report that Hedgehog (Hh) signaling inhibits the formation of BAT during development. Activation of Hh signaling, specifically in the BAT of mice during development, resulted in the loss of interscapular BAT due to the impairment of brown-preadipocyte differentiation. Remarkably, the majority of the BAT cells in the neck were replaced by skeletal muscle-like cells in embryos with elevated Hh activity. These findings indicate that Hh is an essential regulator of BAT development and that developing BAT depots respond differentially to Hh signaling.

Author contributions: L.S. and M.-H.C. designed research; L.N., D.-H.Y., L.S., and M.-H.C. performed research; D.-H.Y., Q.T., and L.S. contributed new reagents/analytic tools; L.N., D.-H.Y., E.J.J., Q.T., L.S., and M.-H.C. analyzed data; and E.J.J., L.S., and M.-H.C. wrote the paper.

The authors declare no conflict of interest.

This article is a PNAS Direct Submission. Y.-H.T. is a guest editor invited by the Editorial Board.

[1]Present address: Harmony School of Science–Houston, Sugarland, TX 77478.

[2]To whom correspondence should be addressed. Email: miaohsuc@bcm.edu.

This article contains supporting information online at www.pnas.org/lookup/suppl/doi:10.1073/pnas.1420978112/-/DCSupplemental.

in differentiating brown FVB-C3 preadipocytes but absent from both proliferating and differentiated mature brown FVB-C3 adipocytes (Fig. 1*A*). Because Hh-pathway components localize to primary cilia after Hh stimulation, we next determined whether brown preadipocytes possess Hh-pathway components and are Hh-responsive. We treated FVB-C3 cells with 1 μM SAG, a Smo agonist, to activate the Hh pathway. Smo, Gli2, and Gli3 all localized to primary cilia upon SAG stimulation in FVB-C3 cells (Fig. 1*B*). Furthermore, both the full-length activator forms of the Gli2 and Gli3 proteins and the repressor form of Gli3 were present in these cells (Fig. 1*C*). Expression of both *Ptch1* and *Gli1* increased after SAG treatment, indicating that the Hh pathway is active in FVB-C3 cells (Fig. 1*D*). We also verified the presence of primary cilia in BAT in vivo by analyzing sections of BAT from both embryonic day 18.5 (E18.5) and postnatal day 14 (P14) mice (Fig. S1*A*). In addition, analysis of primary adipocytes derived from E18.5 BAT confirmed that primary cilia and major Hh-pathway components were present in primary brown preadipocytes upon induction of differentiation and absent from proliferating preadipocytes and mature brown adipocytes (Fig. S1 *B*, *C*, and *D*). Finally, Hh-pathway components were also detected in BAT at E18.5 and P14 by RT-PCR (Fig. 1*E*).

Cell-Autonomous Activation of Hh Signaling Impairs the Development of BAT in Vivo. The precise embryonic stage at which BAT first appears is not clear. Closer investigation revealed that BAT appears by E14.5 and continues to develop until birth (see Fig. S3 *A* and *B*). To investigate the role of Hh signaling in the development of BAT, we conditionally inactivated *Ptch1*, the Hh receptor and a pathway inhibitor, in embryonic BAT because deletion of *Ptch1* induces maximal activation of the Hh pathway (13, 21). Specifically, we used Cre recombinase driven by the *aP2/FABP4* promoter, whose expression is limited to a few embryonic tissues including the neural tube and BAT but not skeletal muscle, to excise $Ptch1^{flox}$ (22) (Fig. S2*A*). *aP2-Cre;* $Ptch1^{flox/-}$ embryos did not seem to be smaller than WT embryos but died at birth most likely due to defects in neural tube-derived tissues (23) (Fig. S2*B*). These embryos almost completely lack BAT in the interscapular region (Fig. S3 *C*, *D*, and *Q*), strongly suggesting that Hh signaling inhibits its development during embryogenesis. To further characterize the in vivo role of Hh in BAT formation, we crossed *aP2-Cre* with the *SmoM2-YFP* allele because Cre-mediated recombination of *SmoM2* results in ligand-independent activation of Hh signaling, which can be tracked by evaluating *YFP* expression (24). These embryos were also of normal size and showed BAT-specific activation of Hh signaling (Fig. S2 *C*, *F*, and *G*). Interscapular BAT was drastically reduced in, but not completely absent from, *aP2-Cre; SmoM2* embryos, further indicating that the Hh pathway inhibits BAT formation (Fig. 2 *A*, *B*, and *C* and Fig. S4*A*). Reduction of BAT mass can result from either reduced brown-adipocyte differentiation or an imbalance between proliferation and apoptosis. Therefore, we used immunohistochemistry (IHC) to compare differentiation and maturation of E18.5 WT and *aP2-Cre; SmoM2* BAT (Fig. 2 *D–O* and Fig. S4*B*). Peroxisome proliferator-activated receptor gamma (PPARγ) and PRD1-BF1-RIZ1 homologous domain containing 16 (PRDM16), two master regulators of brown-adipocyte differentiation, were greatly reduced in BAT sections from the *aP2-Cre; SmoM2* mutant whereas CCAAT/enhancer-binding protein beta (C/EBPβ), another marker for brown preadipocytes, was moderately reduced. Furthermore, uncoupling protein 1 (UCP-1) and adipocyte protein 2 (aP2, also known as FABP4), two crucial regulators of mature brown-adipocyte function, were also decreased in *aP2-Cre; SmoM2* embryos. However, cell proliferation seemed to be normal in *aP2-Cre; SmoM2* mutant BAT (Fig. S5 *A* and *B*). Taken together, our phenotypic analyses indicate that autonomous activation of Hh signaling impairs BAT formation by inhibiting brown-adipocyte differentiation and maturation.

Surprisingly, we also noticed that BAT in the supraclavicular (above the clavicle bone) and ventral neck regions of *aP2-Cre;* $Ptch1^{flox/-}$ and *aP2-Cre; SmoM2* embryos was replaced by a mixture of cells, many of which were either spindled cells or cells morphologically resembling early differentiating skeletal muscle (Fig. 2 *P–S* and Fig. S3 *E–H*). To further investigate the identity of these cells, we first confirmed that cells in this region underwent Cre-mediated recombination and showed increased Hh activation (Fig. S2 *D*, *E*, and *G*) and then evaluated the abundance of key skeletal-muscle markers using IHC. Myogenin, a major skeletal-muscle specification marker, was significantly higher in these cells than in normal muscle cells from WT embryos (Fig. 2 *T* and *U* and Figs. S3 *I*, *J*, and *R* and S4*B*). However, mature skeletal-muscle markers [Desmin and Myosin Heavy Chain (MHC)] were significantly lower (Fig. 2 *V–Y* and Figs. S3 *K–N* and *R* and S4*B*). Furthermore, Ki-67 staining indicated that these cells were highly proliferative. (Fig. 2 *Z* and *A′* and Figs. S3 *O*, *P*, and *R* and S4*B*). Quantitative reverse-transcription PCR (qRT-PCR) analysis of several markers further demonstrated that these cells resemble skeletal-muscle progenitor cells (Fig. S4*C*). Finally, we confirmed that activation of Hh in these mutants did not seem to impede normal skeletal-muscle and dermis development (Fig. S5 *C–E*). Together, these findings suggest that autonomous activation of Hh signaling impairs BAT formation and converts some brown adipose into undifferentiated skeletal-muscle progenitor-like cells.

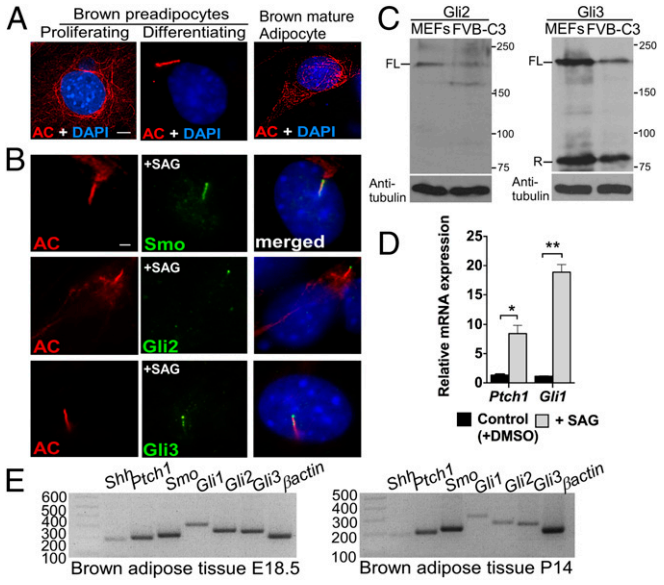

Fig. 1. BAT possesses major Hh-pathway components. (*A*) Immunofluorescence with antibodies against acetylated tubulin (AC; red), a marker for both cytoplasmic microtubules and primary cilium, was performed in proliferating and differentiating brown preadipocytes and in mature brown adipocytes generated from the FVB-C3 cell line ($n = 3$). Staining of the cytoplasmic tubulin network is seen in cells lacking primary cilia, but acetylated tubulin relocalized to the cilium upon assembly, resulting in intense rod-shaped staining. (Scale bar: 5 μm.) (*B*) Double immunofluorescence staining with antibodies against acetylated tubulin (red) and Hh-pathway components Smo, Gli2, and Gli3 (green) in FVB-C3 cells. (Scale bar: 10 μm.) (*C*) Western blot analysis of Gli2 and Gli3 protein abundance in WT embryonic fibroblasts (MEFs) and FVB-C3 cells. α-Tubulin was used as a loading control. FL, full length; R, repressor. (*D*) qRT-PCR analysis of *Ptch1* and *Gli1* in FVB-C3 cells treated with SAG relative to untreated control cells ($n = 3$). Data are presented as mean ± SD. $*P < 0.05$; $**P < 0.01$. (*E*) RT-PCR of *Shh*, *Ptch1*, *Smo*, *Gli1*, *Gli2*, and *Gli3* in BAT isolated from E18.5 WT embryos and 14-d-old pups (P14) ($n = 4$).

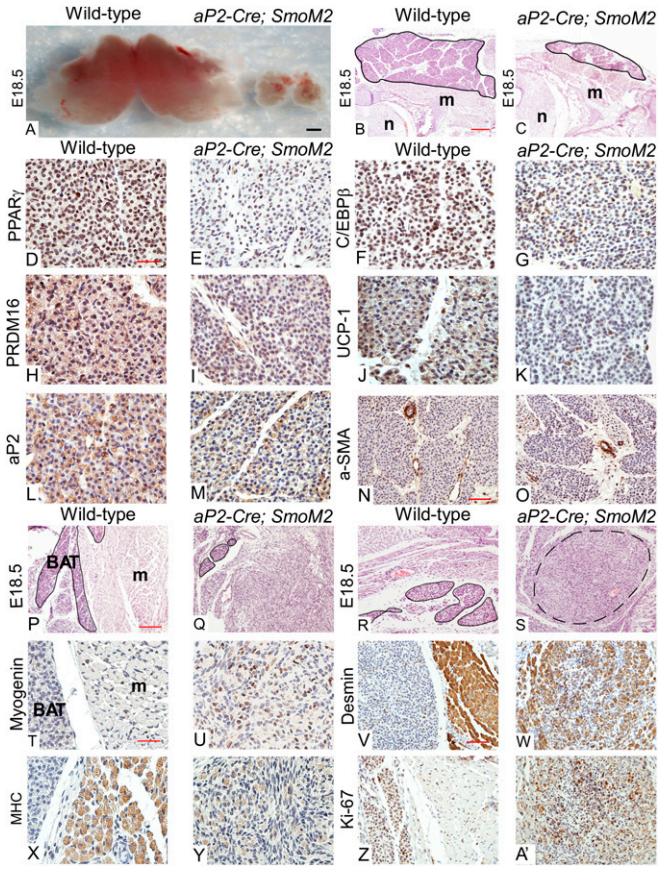

Fig. 2. Hh signaling inhibits BAT development in vivo. (*A*) Intact interscapular BAT dissected from WT and *aP2-Cre; SmoM2* embryos (n = 10 embryos). (Scale bar: 1,000 μm.) (*B* and *C*) H&E-stained E18.5 WT and *aP2-Cre; SmoM2* mouse embryo sections. m, muscle; n, neural tube. Interscapular BAT is outlined in black. (Scale bar: 100 μm.) (*D*–*O*) IHC of E18.5 WT and *aP2-Cre; SmoM2* interscapular BAT sections was performed using antibodies against PPARγ (*D* and *E*), C/EBPβ (*F* and *G*), PRDM16 (*H* and *I*), UCP-1 (*J* and *K*), aP2 (*L* and *M*), and alpha-smooth muscle actin (α-SMA) (*N* and *O*). PPARγ, C/EBPβ, and PRDM16 serve as brown-preadipocyte markers; UCP-1 and aP2 serve as mature brown fat markers; and α-SMA serves as a control (smooth-muscle marker). (Scale bars: *D*–*M*, 25 μm; *N* and *O*, 50 μm.) Quantitative analysis of the images is presented in Fig. S4. (*P*–*S*) H&E-stained E18.5 WT and *aP2-Cre; SmoM2* mouse embryo sections of supraclavicular BAT (*P* and *Q*) and ventral neck BAT (*R* and *S*). BAT is outlined in black. A nodule composed of a mixture of differentiating skeletal muscle and spindled cells is outlined by a black dashed line. (Scale bar: 100 μm.) (*T*–*A′*) IHC of E18.5 WT and *aP2-Cre; SmoM2* supraclavicular brown-adipose sections using antibodies against Myogenin (*T* and *U*), Desmin (*V* and *W*), MHC (*X* and *Y*), and Ki-67 (*Z* and *A′*). (Scale bars: *T, U, X,* and *Y*, 25 μm; *V, W, Z,* and *A′*, 50 μm.) All images shown in this figure are representative of analyses of four embryos per genotype.

Hh Signaling Inhibits Early Brown-Adipocyte Differentiation in Vitro. To more specifically delineate the molecular role of Hh signaling in regulating BAT formation, we generated a brown-preadipocyte cell line (designated BAC-C4) from the stromal-vascular fraction of WT E16.5 interscapular BAT. These cells exhibit a typical spindle-shaped morphology similar to FVB-C3 cells and can be induced to differentiate into mature brown adipocytes using the procedure described in Fig. S6*A*. These cells also contain the machinery required for Hh-pathway activation. Specifically, SAG stimulation resulted in Smo, Gli2, and Gli3 localization to the primary cilia in BAC-C4 cells (Fig. 3*A*), and both full-length activator and repressor forms of Gli proteins were detected in these cells (Fig. 3*B*). In addition, expression of both *Ptch1* and *Gli1* significantly increased after SAG treatment, indicating that BAC-C4 cells were indeed Hh-responsive (Fig. 3*C*). Finally, to test whether activation of the Hh pathway by SAG treatment inhibits adipogenic differentiation, we treated these cells with low (200 nM) and high (1 μM) concentrations of SAG. Brown adipogenic differentiation was completely inhibited by 1 μM SAG treatment (Fig. 3 *D* and *E*). Although this inhibitory effect was less effective in cells treated with a lower concentration of SAG (200 nM), treatment with a natural ligand, Shh, also inhibited differentiation (Fig. S6 *B* and *C*). Expression of brown

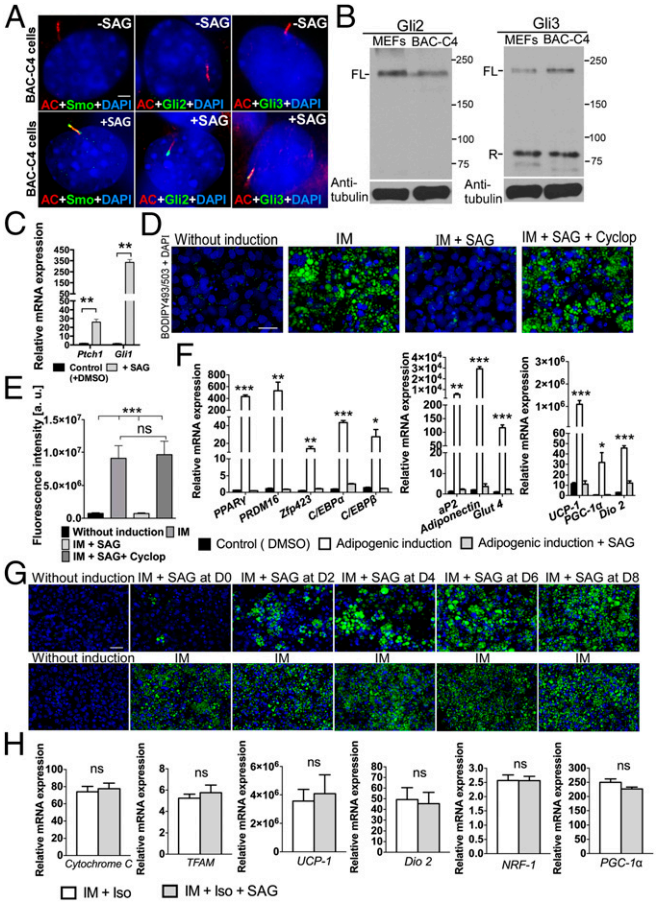

Fig. 3. Hh signaling inhibits brown-adipocyte differentiation. (*A*) Double immunofluorescence staining using antibodies against acetylated tubulin (AC; red) and either Smo, Gli2, or Gli3 (green) in untreated and SAG-treated BAC-C4 cells (n = 3). (Scale bar: 10 μm.) (*B*) Western blot of Gli2 and Gli3 in WT MEFs and BAC-C4 cells. α-Tubulin was used as a loading control. FL, full length; R, repressor. (*C*) qRT-PCR analysis of *Ptch1* and *Gli1* in BAC-C4 cells treated with SAG relative to control cells (n = 3). Data are presented as mean ± SD; $^{**}P < 0.01$. (*D*) BODIPY493/503 staining of BAC-C4 cells cultured with induction medium (IM), with IM and SAG, or with IM, SAG, and Cyclopamine (Cyclop). (Scale bar: 25 μm.) (*E*) Quantitative analysis of BODIPY493/503 staining (fluorescence intensity of images) of BAC-C4 cells (n = 4). Data are presented as mean ± SD; $^{***}P < 0.001$; ns, nonsignificant. (*F*) qRT-PCR analysis of brown-adipocyte differentiation markers (*PPARγ*, *PRDM16*, *Zfp423*, *C/EBPα*, *C/EBPβ*, and *aP2*), mature adipocyte markers (*Adiponectin*, and *Glut4*), and mitochondrial component markers (*UCP-1*, *PGC-1α*, and *Dio2*) in BAC-C4 cells supplemented with IM or with IM and SAG (n = 3). Data are presented as mean ± SD; $^{***}P < 0.001$; $^{**}P < 0.01$; $^{*}P < 0.05$; ns, nonsignificant. (*G*) BODIPY493/503 staining of BAC-C4 cells cultured as outlined in Fig. S6*A*. SAG was added for a 2-d interval at the indicated day after the start of induction (D0, D2, D4, D6, or D8). (Scale bar: 50 μm.) Quantitative analysis of these images is presented in Fig. S6*F*. (*H*) qRT-PCR analysis of genes involved in mitochondrial biogenesis and function in fully differentiated BAC-C4 cells treated with isoproterenol (Iso) or with Iso and SAG at the end of culture period. Data are presented as mean ± SD (n = 3). ns, nonsignificant.

preadipocyte differentiation markers [*PPARγ*, *PRDM16*, zinc finger protein 423 (*Zfp423*), CCAAT/enhancer-binding protein alpha (*C/EBPα*), and *C/EBPβ*], terminal differentiation markers [*aP2*, *Adiponectin*, and glucose transporter type 4 (*Glut4*)], and mitochondrial function markers [*UCP-1*, PPARγ coactivator 1-alpha (*PGC-1α*), and type II iodothyronine deiodinase (*Dio2*)] significantly increased after adipogenic induction, and this increase was largely inhibited by SAG treatment (Fig. 3*F*). Applying cyclopamine, an Hh-pathway inhibitor, alone did not affect adipogenesis of BAC-C4 cells (Fig. S7). However, when we applied cyclopamine to SAG-activated BAC-C4 cells, the inhibitory effect of SAG was completely reversed (Fig. 3 *D*, *E*, and *F*). These results strongly support the notion that Hh signaling negatively regulates brown-preadipocyte differentiation.

Brown adipogenesis can be divided into early differentiation (marked by up-regulation of proadipogenic genes) and terminal differentiation (marked by accumulation of lipid droplets and by up-regulation of genes regulating mitochondrial function). To further delineate the role of Hh signaling in brown adipogenesis, we defined the window during differentiation wherein brown preadipocytes were most sensitive to Hh. Brown-preadipocyte differentiation was primarily blocked by SAG treatment during the first 2 d of adipogenic induction (Fig. 3*G* and Fig. S6 *D–F*). The inhibitory effect of Hh signaling diminished as adipogenesis proceeded and was no longer observed when SAG treatment was applied after 4 d of induction (Fig. 3*G* and Fig. S6 *D–F*), indicating that the early stages of differentiation are more sensitive to Hh inhibition. Furthermore, the induction of Hh target genes in response to SAG treatment was much higher in early differentiating brown preadipocytes than in brown adipocytes that were nearly terminally differentiated (Fig. S6 *G* and *H*). Finally, activation of Hh signaling did not directly inhibit expression of genes involved in mitochondrial biogenesis and function in fully differentiated BAC-C4 cells (Fig. 3*H*). Thus, the reduction of mature brown-adipocyte and mitochondrial markers in SAG-treated BAC-C4 cells is likely due to the indirect effects of suppression of early differentiation by the Hh pathway.

To further confirm that activation of the Hh pathway inhibits brown adipogenesis, we generated another brown-preadipocyte cell line (designated SmoM2) isolated from the interscapular BAT of E16.5 *aP2-Cre; SmoM2* mutants. The Hh pathway is autonomously activated in SmoM2 cells (Fig. S8*A*), greatly hampering the ability of these cells to differentiate into mature brown adipocytes (Fig. S8 *B–D*). We reasoned that, if activation of the Hh pathway inhibits BAC-C4–cell differentiation, reduction of Hh-pathway activity in SmoM2 cells should restore differentiation. Because cyclopamine has very low affinity for the mutated Smo receptor and thus fails to inhibit Hh activity in cells with the *SmoM2* mutation (25, 26) (Fig. S9*A*), we used another Hh-pathway inhibitor, SANT-1, to test this hypothesis (26). Expression of both *Ptch1* and *Gli1* was reduced in SAG-activated BAC-C4 cells and in SmoM2 cells that were treated with SANT-1, indicating that SANT-1 can effectively inhibit Hh-pathway activity in these two cell lines (Fig. S9 *A* and *B*). More importantly, SANT-1 restored brown adipogenic differentiation in BAC-C4 cells treated with SAG and in SmoM2 cells (Fig. S9 *C* and *D*). Finally, knockdown of *Sufu,* one of the Hh-pathway components downstream of Smo, reduced Hh-pathway activity and partially restored brown adipogenesis in SmoM2 cells (Fig. S10). Collectively, these data strongly support an inhibitory role for Hh in brown adipogenesis.

Hh Signaling Inhibits Brown-Preadipocyte Differentiation Partially Through Up-Regulation of *COUP-TFII*. Hh signaling regulates developmental processes by modulating expression of downstream target genes. To search for target genes involved in the Hh response, we examined the expression of known anti-adipogenic genes [*Necdin*, *COUP-TFII*, GATA binding protein 2 (*GATA2*), GATA binding protein 3 (*GATA3*), wingless-type MMTV integration site family, member 10B (*Wnt10b*), and preadipocyte factor-1 (*Pref-1*)] and of genes involved in determination of bone [runt-related transcription factor 2 (*Runx2*)] and skeletal muscle (*MyoD1* and *Myogenin*) cell fate in SmoM2 cells. Our analysis showed that SmoM2 cells showed increased mRNA expression of *COUP-TFII*, an Hh target gene that inhibits white-preadipocyte differentiation (Fig. 4*A*) (27, 28). COUP-TFII protein levels were also up-regulated both in SmoM2 cells and in FVB-C3 cells treated with SAG, but this up-regulation was much higher in SmoM2 cells (Fig. 4*B*). In addition, COUP-TFII–protein abundance inversely correlated with the extent of brown-preadipocyte differentiation (Fig. 4*C*), suggesting that COUP-TFII acts early in brown-adipocyte differentiation.

Because both our in vivo and in vitro studies indicated that the Hh pathway suppresses brown adipogenesis and that *COUP-TFII* expression is up-regulated by Hh, we hypothesized that Hh elicits its inhibitory effects by up-regulating COUP-TFII expression in brown preadipocytes. To test this hypothesis, we generated BAC-C4 cells that either overexpress *COUP-TFII* or express shRNA against *COUP-TFII* (*shCOUP-TFII*) (Fig. 4*D*). Brown-preadipocyte differentiation was blocked in BAC-C4 cells overexpressing *COUP-TFII*, and cyclopamine was no longer able to reverse Hh-mediated suppression of brown adipogenesis in these cells (Fig. 4 *E* and *F*). By contrast, BAC-C4 cells expressing *shCOUP-TFII* showed higher lipid-droplet accumulation, an indication of the degree of adipocyte differentiation, than cells expressing the *shLuc* control (Fig. 4 *G* and *H*). Furthermore, *shCOUP-TFII* partially reversed the inhibitory effect of SAG treatment on adipocyte differentiation by causing a moderate, but significant, increase in the expression of genes regulating early differentiation, lipid production, and thermogenesis (Fig. 4 *G*, *H*, and *I*). Together, these data indicate that knockdown of *COUP-TFII* results in a partial rescue of brown adipogenesis in SAG-treated BAC-C4 cells. A recent study identified potential Gli-binding sites on the *COUP-TFII* promoter and showed that promoter activity increased after cotransfection with Gli transcription factors in white preadipocytes (3T3-L1 cells), suggesting that *COUP-TFII* is a direct Hh target gene mediating the inhibitory effects of Hh in white adipogenesis (19). To test whether *COUP-TFII* expression is directly activated in response to Hh signaling in brown preadipocytes, we cotransfected BAC-C4 cells with Gli expression constructs and a reporter construct containing a Luciferase gene regulated by a *COUP-TFII* promoter that contained these Gli-binding sites. The Gli2 expression construct generated a modest but significant increase in *COUP-TFII*–promoter activity, indicating that Gli2 may mediate the transcriptional activation of *COUP-TFII* (Fig. 4*J*). Therefore, we also tested the ability of Gli2 to directly bind to the endogenous *COUP-TFII* promoter by chromatin immunoprecipitation (ChIP) of SmoM2 and BAC-C4 cells. Gli2 directly bound the endogenous *COUP-TFII* promoter in SmoM2 cells, but not in non–Hh-stimulated BAC-C4 cells (Fig. 4*K*). Finally, COUP-TFII immunostaining is higher in *aP2-Cre; SmoM2* embryos than in WT embryos (Fig. 4 *L* and *M*). Collectively, our studies show that COUP-TFII is a direct Hh target gene that can partially suppress Hh-mediated brown adipogenesis.

Discussion

In this study, we provide, to our knowledge, the first in vivo evidence that Hh signaling plays a negative role in BAT development. We show that BAT formation is severely perturbed in both *aP2-Cre; Ptch1$^{flox/-}$* and *aP2-Cre; SmoM2* mice. These observations conflict with those of Pospisilik et al., who reported that WAT but not BAT was inhibited by activation of the Hh pathway in *aP2-Cre; Sufu* mice (19). We postulate that the difference between their observations and ours is because, unlike deleting *Ptch1* or using constitutively active *SmoM2*, inactivation of *Sufu* may not result in maximal activation of the Hh pathway

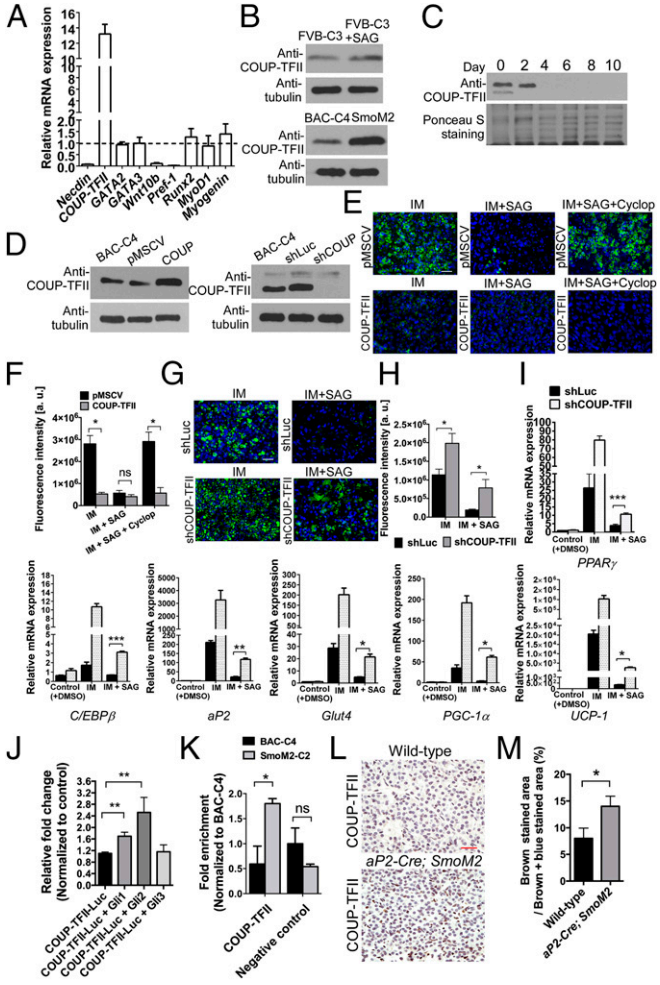

Fig. 4. Hh signaling inhibits brown adipocyte differentiation by increasing *COUP-TFII* expression in brown preadipocytes. (*A*) qRT-PCR analysis of negative regulators of adipogenesis (*Necdin*, *COUP-TFII*, *GATA2*, *GATA3*, *Wnt10b*, and *Pref-1*) and of bone (*Runx2*) and skeletal muscle (*MyoD1* and *Myogenin*) specific genes in SmoM2 cells relative to expression in untreated BAC-C4 cells. Data are presented as mean ± SD ($n = 3$). (*B*) Western blot analysis of COUP-TFII abundance in FVB-C3, BAC-C4, and SmoM2 cells ($n = 4$). COUP-TFII was normalized to α-tubulin. (*C*) Western blot analysis of COUP-TFII in BAC-C4 cells throughout the course of the 10-d differentiation period described in Fig. S6*A*. Ponceau S Staining was used to confirm loading of equivalent amounts of protein ($n = 4$). (*D*) Western blot analysis of COUP-TFII in BAC-C4 cells expressing retroviral pMSCV-*COUP-TFII* (COUP), pMSCV (empty vector, control), shRNA against *COUP-TFII* (shCOUP), and shRNA against *Luciferase* (shLuc, control). (*E*) BODIPY493/503 staining of BAC-C4 cells expressing the empty retroviral pMSCV vector or retroviral *COUP-TFII*. Cells were cultured with IM, IM and SAG, or IM, SAG, and Cyclopamine (Cyclop) ($n = 4$). (Scale bar: 50 μm.) (*F*) Quantitative analysis of BODIPY493/503 staining in BAC-C4 cells containing either pMSCV or retroviral *COUP-TFII*. Data are presented as mean ± SD ($n = 4$). $^*P < 0.05$; ns, nonsignificant. (*G*) BODIPY493/503 staining of BAC-C4 cells expressing *shLuc* or *shCOUP-TFII* ($n = 4$). (Scale bar: 50 μm.) (*H*) Quantitative analysis of BODIPY493/503 staining in BAC-C4 cells expressing *shLuc* or *shCOUP-TFII*. Data are presented as mean ± SD ($n = 4$). $^*P < 0.05$. (*I*) qRT-PCR analyses of brown-adipocyte differentiation markers in BAC-C4 cells expressing *shLuc or shCOUP-TFII*. Data are presented as mean ± SD; $^{***}P < 0.001$, $^{**}P < 0.01$, $^*P < 0.05$. (*J*) The Gli2 expression construct activates Luciferase reporter gene expression driven by a *COUP-TFII* promoter containing Gli binding sites ($n = 3$). Data are presented as mean ± SD; $^{**}P < 0.01$. (*K*) ChIP analysis of Gli2 binding to the *COUP-TFII* promoter in BAC-C4 and SmoM2 cells. Data are presented as mean ± SD; $^*P < 0.05$; ns, nonsignificant. (*L*) IHC of E18.5 WT and *aP2-Cre; SmoM2* brown adipose sections using antibodies against COUP-TFII ($n = 4$). (Scale bar: 25 μm.) (*M*) Quantitative analysis of COUP-TFII–positive staining in WT and *aP2-Cre; SmoM2* brown-adipose sections. Data are presented as mean ± SD ($n = 4$ embryos); $^*P < 0.05$.

(13, 14). In fact, knockdown of *Sufu* actually reduced Hh pathway activity in SmoM2 cells enough to partially restore brown-preadipocyte differentiation. Furthermore, our in vitro experiments with 1 μM SAG show that Hh signaling directly inhibits differentiation of WT brown preadipocytes whereas SAG is less effective at inhibiting differentiation at the lower concentration (200 nM) used by Pospisilik et al. Conversely, inhibition of the Hh pathway with Cyclopamine (BAC-C4 cells) or SANT-1 (BAC-C4 and SmoM2 cells) reduced Hh-pathway activity and restored differentiation.

Although these studies show that Hh signaling negatively regulates BAT development, Hh also positively regulates the specification and maintenance of the epaxial dermomyotome and of *Myf5* expression during early myogenesis (11). Recent studies indicated that the developmental fates of BAT and skeletal muscle ($Myf5^+$ cells) are closely related; both lineages are derived from the dermomyotome (9, 10). We observed that high Hh-pathway activity might redirect some brown preadipocytes (in the ventral neck and supraclavicular BAT) toward a skeletal-muscle cell fate in both *aP2-Cre; Ptch1$^{flox/-}$* and *aP2-Cre; SmoM2* mutants. Intriguingly, our marker analyses indicated that these cells more closely resemble skeletal-muscle progenitor cells than differentiated myotubes because greater amounts of Myogenin and lower amounts of Desmin and MHC are present in these cells than in differentiated muscle cells from WT embryos. These observations suggest that Hh-signaling activity may potentially serve as a switch that inhibits BAT and promotes skeletal-muscle fate determination. The possibility of an Hh-mediated BAT/skeletal muscle fate switch was also recently proposed by Hatley et al. Using a new *aP2-Cre* line generated by Tang et al. (distinct from the line used in this study), these authors showed that autonomous activation of Hh signaling in the brown-adipocyte lineage results in the appearance of embryonal rhabdomyosarcoma, an aggressive skeletal muscle tumor, in postnatal mice (29, 30).

Even though the results of our studies support a role for the Hh pathway in regulating a BAT/skeletal-muscle fate switch, only the BAT depots in the ventral neck and supraclavicular regions were transformed into immature skeletal muscle whereas interscapular BAT in the more dorsal region was not. This difference suggests that the ability of brown preadipocytes to be redirected toward the skeletal-muscle fate is context-dependent and likely involves other extracellular signals in addition to the Hh pathway.

Hh signaling exerts its effects through repression/activation of downstream target genes. *COUP-TFII*, a nuclear orphan receptor of the steroid-thyroid hormone receptor subfamily and a direct Hh target gene, is expressed widely in the developing mouse embryo and controls multiple components of embryonic patterning (28, 31). In this study, we found that *COUP-TFII* is upregulated by Hh-pathway activity in brown preadipocytes, suggesting that COUP-TFII may also play a role in brown adipogenesis. Indeed, our in vitro studies showed that brown-preadipocyte differentiation is inhibited by overexpression of *COUP-TFII* and is enhanced by knockdown of *COUP-TFII*. Recently, COUP-TFII was found to suppress white adipogenesis, likely through interaction with GATA2 (27). Surprisingly, the expression of both *GATA2* and *GATA3* was not significantly altered in SmoM2 cells (Fig. 4*A*), suggesting that COUP-TFII may regulate brown adipogenesis through interactions with other cofactors.

Embryonic tissue patterning is orchestrated by a network of secreted signaling molecules that needs to be tightly controlled. Perturbation of signaling molecules in this network can result in catastrophic events leading to embryonic lethality or diseases in adulthood. Given that the same precursor cells giving rise to BAT also give rise to skeletal muscle, the balance between signaling molecules that both positively and negatively regulate cell fate is critical for proper development of these tissues. Here, we show that perturbation of Hh signaling in BAT during development can severely impair the formation of BAT, an embryonic tissue that is critical for survival of neonates and adult energy homeostasis. To further define the role of Hh signaling in

BAT formation, future studies should focus on manipulating Hh-pathway activity during embryonic myogenesis and investigating the relationship between Hh, COUP-TFII, and other signaling pathways in regulating BAT development.

Materials and Methods

Materials. A detailed description of materials used in these studies is included in *SI Materials and Methods*.

Animals. Mouse husbandry and embryo collection procedures were approved by the Institutional Animal Care and Use Committee at Baylor College of Medicine, Houston.

Embryonic Brown-Preadipocyte Cell-Line Generation and Differentiation. Primary brown preadipocytes (stromal-vascular fraction) were isolated by collagenase digestion of interscapular BAT from E16.5 WT and *aP2-Cre; SmoM2* mouse embryos. These primary cells were subsequently immortalized following a previously described method (13). The procedure to induce brown preadipocytes to differentiate is provided in *SI Materials and Methods*.

Embryo Processing and Histology. Embryos were fixed in 4% (wt/vol) paraformaldehyde, dehydrated in ethanol, and cleared in toluene before embedding in paraffin and sectioning. H&E staining was performed using standard procedures.

Immunofluorescence. Immunofluorescence of histological sections and cultured cells is detailed in *SI Materials and Methods*. Images were captured using a CoolSNAP$_{ES}^2$ camera connected to a Nikon Eclipse 80i stereomicroscope and processed using the NIS Elements AR 3.2 Nikon imaging software.

Immunohistochemistry. Immunohistochemistry of histological sections is detailed in *SI Materials and Methods*.

Western Blot. SDS/PAGE and Western blotting were performed as previously described (13).

RNA Isolation, RT-PCR, and qRT-PCR Analysis. Total RNA was first extracted by homogenizing the cell pellets with TRIzol (Invitrogen), followed by using the RNAeasy Mini Kit (Qiagen). cDNA was reverse transcribed using SuperScript III Reverse Transcriptase (Invitrogen). qPCR was performed in triplicate. Primer sequences used for RT-PCR are listed in Table S1. Primer sequences used for qRT-PCR are listed in Table S2. RT-PCR details are provided in *SI Materials and Methods*.

BODIPY 493/503 Staining. Cells were rinsed twice in PBS, fixed with 4% paraformaldehyde for 30 min, and stained with BODIPY 493/503 diluted in PBS (1:1,000; Sigma) for another 30 min. Cells were counterstained with DAPI.

Retroviral Production and Generation of Stable Cell Lines. HEK 293T cells were transfected with pCL-ECO and pMSCV-COUP-TFII or pMSCV empty vector using Lipofectamine 2000 (Invitrogen) as previous described (13). Stable expression of COUP-TFII was verified by Western blotting.

Lentiviral Production and Generation of Stable Cell Lines. Short-hairpin RNA (shRNA) plasmids were constructed, and lentiviral particles were produced following the standard pLKO.1 cloning protocol detailed in *SI Materials and Methods*.

Luciferase Assays. A previously identified fragment [NM183261; −3,958 bp to −2,686 bp relative to the *COUP-TFII* transcription start site (TSS)] (19) from the *COUP-TFII* promoter was cloned into a pGL3-basic vector to generate the COUP-TFII reporter construct. A full description of the Luciferase assay is provided in *SI Materials and Methods*.

Chromatin Immunoprecipitation and Real-Time PCR. ChIP analyses are described in *SI Materials and Methods*. Primer and probe sets to generate products containing the region of predicted Gli binding (−3,167 bp to −3,159 bp) at the COUP-TFII promoter and the negative control regions are summarized in Table S3.

Statistical Analyses. The Student's *t* test and Mann–Whitney method were used to evaluate statistical significance between two groups. One-way ANOVA and the Kruskal—Willis method were used to evaluate statistical significance between three or more groups. Unless specified, the following apply: $***P < 0.001$, $**P < 0.01$, $*P < 0.05$, and nonsignificant (ns), $P > 0.05$. Prism 6 software was used to perform statistical analyses and generate graphs.

ACKNOWLEDGMENTS. We thank Drs. Evan Rosen, Inder Verma, Bob Weinberg, David Root, Didier Trono, Ronald Evans, Matthew Scott, Andrew McMahon, Philippe Soriano, and Pao-Tien Chuang for reagents and animals; Alexis Canlas and Chitra Jeyasankar for technical assistance; and Dr. Ray-Bing Chen for helpful discussions regarding the statistical analyses. This work was supported by a grant (6250-51000-054) from the US Department of Agriculture/Agricultural Research Service (to M.-H.C.).

1. Gesta S, Tseng YH, Kahn CR (2007) Developmental origin of fat: Tracking obesity to its source. *Cell* 131(2):242–256.
2. Virtanen KA, et al. (2009) Functional brown adipose tissue in healthy adults. *N Engl J Med* 360(15):1518–1525.
3. Cypess AM, et al. (2009) Identification and importance of brown adipose tissue in adult humans. *N Engl J Med* 360(15):1509–1517.
4. Saito M, et al. (2009) High incidence of metabolically active brown adipose tissue in healthy adult humans: Effects of cold exposure and adiposity. *Diabetes* 58(7): 1526–1531.
5. van Marken Lichtenbelt WD, et al. (2009) Cold-activated brown adipose tissue in healthy men. *N Engl J Med* 360(15):1500–1508.
6. Carey AL, et al. (2013) Ephedrine activates brown adipose tissue in lean but not obese humans. *Diabetologia* 56(1):147–155.
7. Tseng YH, et al. (2008) New role of bone morphogenetic protein 7 in brown adipogenesis and energy expenditure. *Nature* 454(7207):1000–1004.
8. Seale P, Kajimura S, Spiegelman BM (2009) Transcriptional control of brown adipocyte development and physiological function—of mice and men. *Genes Dev* 23(7):788–797.
9. Atit R, et al. (2006) Beta-catenin activation is necessary and sufficient to specify the dorsal dermal fate in the mouse. *Dev Biol* 296(1):164–176.
10. Lepper C, Fan CM (2010) Inducible lineage tracing of Pax7-descendant cells reveals embryonic origin of adult satellite cells. *Genesis* 48(7):424–436.
11. Borycki AG, et al. (1999) Sonic hedgehog controls epaxial muscle determination through Myf5 activation. *Development* 126(18):4053–4063.
12. Wilson CW, Chuang PT (2010) Mechanism and evolution of cytosolic Hedgehog signal transduction. *Development* 137(13):2079–2094.
13. Chen MH, et al. (2009) Cilium-independent regulation of Gli protein function by Sufu in Hedgehog signaling is evolutionarily conserved. *Genes Dev* 23(16):1910–1928.
14. Liu J, Heydeck W, Zeng H, Liu A (2012) Dual function of suppressor of fused in Hh pathway activation and mouse spinal cord patterning. *Dev Biol* 362(2):141–153.
15. Wang C, Pan Y, Wang B (2010) Suppressor of fused and Spop regulate the stability, processing and function of Gli2 and Gli3 full-length activators but not their repressors. *Development* 137(12):2001–2009.
16. Huangfu D, et al. (2003) Hedgehog signalling in the mouse requires intraflagellar transport proteins. *Nature* 426(6962):83–87.
17. Corbit KC, et al. (2005) Vertebrate Smoothened functions at the primary cilium. *Nature* 437(7061):1018–1021.
18. Rohatgi R, Milenkovic L, Scott MP (2007) Patched1 regulates hedgehog signaling at the primary cilium. *Science* 317(5836):372–376.
19. Pospisilik JA, et al. (2010) Drosophila genome-wide obesity screen reveals hedgehog as a determinant of brown versus white adipose cell fate. *Cell* 140(1):148–160.
20. Klein J, et al. (1999) beta(3)-adrenergic stimulation differentially inhibits insulin signaling and decreases insulin-induced glucose uptake in brown adipocytes. *J Biol Chem* 274(49):34795–34802.
21. Méthot N, Basler K (2001) An absolute requirement for Cubitus interruptus in Hedgehog signaling. *Development* 128(5):733–742.
22. Urs S, Harrington A, Liaw L, Small D (2006) Selective expression of an aP2/Fatty Acid Binding Protein 4-Cre transgene in non-adipogenic tissues during embryonic development. *Transgenic Res* 15(5):647–653.
23. Goodrich LV, Milenković L, Higgins KM, Scott MP (1997) Altered neural cell fates and medulloblastoma in mouse patched mutants. *Science* 277(5329):1109–1113.
24. Mao J, et al. (2006) A novel somatic mouse model to survey tumorigenic potential applied to the Hedgehog pathway. *Cancer Res* 66(20):10171–10178.
25. Taipale J, et al. (2000) Effects of oncogenic mutations in Smoothened and Patched can be reversed by cyclopamine. *Nature* 406(6799):1005–1009.
26. Chen JK, Taipale J, Young KE, Maiti T, Beachy PA (2002) Small molecule modulation of Smoothened activity. *Proc Natl Acad Sci USA* 99(22):14071–14076.
27. Xu Z, Yu S, Hsu CH, Eguchi J, Rosen ED (2008) The orphan nuclear receptor chicken ovalbumin upstream promoter-transcription factor II is a critical regulator of adipogenesis. *Proc Natl Acad Sci USA* 105(7):2421–2426.
28. Krishnan V, et al. (1997) Mediation of Sonic hedgehog-induced expression of COUP-TFII by a protein phosphatase. *Science* 278(5345):1947–1950.
29. Hatley ME, et al. (2012) A mouse model of rhabdomyosarcoma originating from the adipocyte lineage. *Cancer Cell* 22(4):536–546.
30. Tang W, et al. (2008) White fat progenitor cells reside in the adipose vasculature. *Science* 322(5901):583–586.
31. Takamoto N, et al. (2005) COUP-TFII is essential for radial and anteroposterior patterning of the stomach. *Development* 132(9):2179–2189.